RADIAL LIP SEALS EFFICIENCY UNDER DYNAMIC OPERATING CONDITIONS

M. SILVESTRI, E.PRATI, A.TASORA

Università degli Studi di Parma, Dipartimento di Ingegneria Industriale
Parco Area delle Scienze, 43100 Parma, Italy
`silve@ied.unipr.it, prati@ied.unipr.it, tasora@ied.unipr.it`

ABSTRACT

This paper describes experimental and numerical procedures to estimate friction torque on a rotating shaft due to radial elastomeric seals. Two different test rigs have been built, in order to highlight the relationship between the overall friction and the local behaviour of each lip portion in presence of dynamic eccentricities. A direct measurement has been performed with a rotating shaft machine and results have been compared with the torque calculated as product of a global frictional coefficient and the normal stress on the lip surface. The latter has been computed by an improved FEM simulation which has been specifically optimized in order to evaluate the lip deformation due to mounting interference. Previous experimental results about radial and tangential oscillation of a limited lip region allowed to calculate the frictional coefficient as the ratio of the friction force and the force pressing the lip on the shaft surface.

KEYWORDS Rotating shafts, Seals, Friction, Efficiency.

NOMENCLATURE

ε:	strain	F_f:	friction force
ε_r:	radial strain	N:	normal force
ε_r:	tangential strain	f:	friction coefficient
ρ:	density	e_d:	dynamic eccentricity
σ:	tensile stress	e_s:	static eccentricity
ω:	shaft speed	k:	spring constant
A:	section area	l:	lenght deformed spring
E:	modulus of elasticity	l_0:	lenght undeformed spring
F:	force	x:	spring elongation

1 INTRODUCTION

This paper describes the latest developments in a research that has been carried on during several years in the Industrial Engineering Department of Parma, with the final aim to satisfactorily explain the behaviour of radial lip seals at varying shaft speed and other operating conditions.

In particular, the increasing importance of energy efficiency, caused by both cost and environmental issues, suggested to deepen the influence factors for friction, in the light of previous experimental results.

Radial lip seals for rotating shafts are largely used both to prevent internal system fluids from leaking and to keep external contaminants from entering the system. Lip seals consist of an elastomer ring equipped with a strenghtening metallic insert. The ring ends, at shaft interface, with a lip. A garter spring stiffens the lip, ensures a better uniformity degree of the bearing pressure and increases the radial interference between seal and shaft on varying working conditions.

Investigations on the sealing and lubrication of radial lip seals have a long tradition [1], [2], [3], involving different disciplines as hydrodynamics, materials science and tribology. Their behaviour has been explained with the influence of temperature [4] and visco-elastohydrodinamic lubrication [5], [6], but such explanations do not completely justify experimental results [7] [8].

Preceding works have shown many experimental results achieved both in working conditions and with simulation apparatus by means of several transducers: cameras, torque meters, accelerometers (for *Frequency Response Function analysis*), thermocouples, flow measurements and, recently, a strain gauge transducer mounted on a machine that simulates actual operating conditions [9], [10].

This work is aimed at establishing a connection between numerical and experimental investigations, useful to properly evaluate pressing force and frictional coefficient contributions to resistant torque on the shaft at different temperatures and shaft speeds.

2 TORQUE DIRECT MEASUREMENT

Measuring overall friction between rotating shaft and radial seals has been performed by means of a few simple changes on a previously built test rig.

The test machine originally was made up by a rotating shaft with, at the end, a disk of circular profile which is in contact with the test seal. The seal was mounted on a fixed housing in order to contain the oil within the crankcase.

Last changes consist in interposing, between crankcase and flange, a ball bearing, so that the flange is free to rotate because of the shaft dragging on the seal.

This degree of freedom is eliminated by a constraint consisting in a custom load cell, made up by a metal cantilever on which two strain gauges are glued. This cantilever has one end fixed on the machine chassis, while the other one blocks the flange with the lip seal.

When the shaft starts to move, friction causes dragging on the seal. This force is transmitted to the flange and then flexes the cantilever, causing a signal on the strain gauge conditioning amplifier.

This signal, with proper calibration (see Figure: 1, gives a reliable measurement ($\pm 4\%$) of the overall friction forces acting on the shaft due to the radial seal.

The used specimens were VITON$^{\circledR}$, 70x110x12 seals. The machine setup was aimed at limiting the effects of eccentricities: the dynamic one was set to $0.05\ mm$, while the static one was limited to $0.1\ mm$.

Tests were performed at varying shaft speed between 300 and 3100 rpm. The corresponding results (see Figure: 2) show a maximum, near 500 rpm, then the friction torque decreases and remain in practice constant up to 2500 rpm, when starts to increase again.

3   NORMAL STRESS

Friction torque can be seen as product of the normal stress on the lip-shaft contact surface and an overall average friction coefficient which depends on shaft speed and lubricating conditions.

In order to properly evaluate the normal stress, a new FEM analysis model has been performed using the ABAQUS software suite. It draws on the model illustrated in [10] and [11] with a few important improvements.

In particular, a new procedure has been adopted for the first analysis step, which identifies the elastomer strains due to mounting interference. Unlike in [11], it is calculated by modelling the shaft as a cylindrical body and the garter spring as a toroidal body and forcing the assembly causing the rubber deformation.

The garter spring is modelled with a homogeneous, elastic, body, whose modulus of elasticity has been calculated so that its value does not change passing from the complex garter spring structure to the simple toroidal shape.

For this purpose, we combine the well-known equation which states that the strain is linearly related to the force (where F is the force causing the deformation):

$$F = k \cdot x \tag{1}$$

with the elastic behaviour of the toroid:

$$\sigma = E \cdot \varepsilon \tag{2}$$

Let elogations are equal in both cases ($\varepsilon \cdot l_0 = x$) and:

$$\varepsilon = \frac{l - l_0}{l_0} \tag{3}$$

observing:

$$\sigma = \frac{F}{A} \tag{4}$$

results:

$$F = A \cdot \sigma = A \cdot E \cdot \varepsilon \tag{5}$$

and finally:

$$E = \frac{k \cdot l_0}{A} \tag{6}$$

Using parameters: $k = 0,95 N/mm$, $l_0 = 240mm$ and $A = 240mm^2$, it results, for the toroidal body, $E = 50.4 N/mm^2$. Its model is made up by hexaedric, linear, 8-nodes elements (C3D8R). The shaft is simply modelled as an *analytical rigid* body, being its deformation neglegible.

The main part of the seal, consisting in the elastomeric ring, has been modelled following the solution illustrated in [10], aiming at reducing complexity and computation time. As shown in figure 3, the ring is divided in two parts, so in the most important one (near the contact with the shaft) the elements are smaller. They are linear, hybrid, hexaedric 8-nodes (C3D8RH).

The three bodies are assebled as shown in figure 4, with the external surface of the rubber ring is blocked, while the spring and the lip are jointed with the *tie* option.

The contact area between shaft and lip is a cylindrical surface 75 μm long [5] lying on the shaft. The lip strain is simulated through three steps: in the first one, the shaft is blocked (*encastre* option) and the relative position of the lip is forced, so that the lip should penetrate the shaft. Then the ABAQUS solving engine deforms the lips determining the effect of the mounting interference (equal to $0.7mm$).

Further, a rigid displacement of the shaft along a direction ortoghonal to the shaft axis simulates a certain static eccentricity, which has been fixed equal to $0.2mm$ in order to ease comparing the results with previous studies [11].

Finally, the shaft is rotated around an axis parallel to the shaft's one, so that a dynamic eccentricity is considered. This parameter is varied between 0 and 0.4 mm, in order to highlight its influence. The shaft speed ω has been set to 1000 rpm.

The normal stress on the lip surface is shown in figure 5 and 6. They agree with the diagram obtained in [5], quoted in figure 7. The overall lip stress at a fixed instant of time, in presence of both static and dynamic eccentricity, is shown in figure 8.

The influence of dynamic eccentricity is highlighted in figure 9 and 10: one can note the effect of viscoelastic material behaviour increases the average stress when the eccentricity becomes larger.

On basis of experimental data reported in the previous paragraph (see Figure: 2) and according with a few data available in literature ([12] and [13]), the lubricated friction coefficient has been drawn equal to 0.23, allowing to calculate the friction torque at varying ε_d as shown in figure 11.

4 STRAIN AND FRICTION

Previous papers [9], [10] and [11] presented a custom strain gauge transducer useful to measure the lip strain in the region close to the shaft surface, aimed at deepening the process of clearance forming between lip and shaft. The same instrument can be used for obtaining the radial and tangential lip strain in standard working conditions. Figure 12 shows an example of data acquisition at 350 rpm: the signal is reported without filtering nor interpolation. The same data che be collected on both axes of single diagram, generating the so-called *Lissajous figures* [9], as shown in figure 13.

These measures are related to the voltage which indicates the cantilever flexion through the equation 2. Let's suppose that stress and strain are linear dependent, then is possible to refer the generic friction coefficient definition:

$$f = \frac{F_f}{N} \tag{7}$$

to this specific case, obtaining:

$$f = \varepsilon_t \cdot \varepsilon_r \tag{8}$$

In order to properly interpret the results, the Lissajous figures (see Figure 13) have been interpolated with the best fitting ellipses (see Figure 14). The ellipses major axis slope (see Figure: 15) corresponds, from an experimental point of view, to the friction coefficient definition given by the equation 8.

Repeating data acquisition and analysis seen in figures 12, 13, 14 and 15 in the range of $100 \div 1100\ rpm$ with step of $50\ rpm$, a friction coefficient diagram can be drawn (see Figure: 16). It increases at low speed, sharply decreases over $500\ rpm$ and then it increases again, qualitatively agreeing with the result numerically obtained by [12].

The normal stress diagram illustrated in the previous paragraph and this indirect measure of the friction coefficient allow to estimate the friction torque as a function of the local lip strains. The torque diagram is shown in figure 17, compared with the direct torque measure seen at the paragraph 2. These results agree satisfactorily among themselves.

5 CONCLUSION

Experimental and numerical procedures to estimate the friction torque due to radial elastomeric seals have been illustrated. Two different test rigs allowed to highlight the relationship between the overall friction and the local behaviour of each lip portion, also in presence of dynamic eccentricities. A direct measurement has been performed with a rotating shaft machine and results have been compared with the torque calculated as product of a global frictional coefficient and the normal stress on the lip surface. The latter has been computed by an improved FEM simulation which has been specifically optimized in order to evaluate the lip deformation due to mounting interference. Previous experimental results about radial and tangential oscillation of a limited lip region allowed to calculate the frictional coefficient as the ratio of the friction force and the force pressing the lip on the shaft surface. Numerical results agree with experimental ones and with numerical models available in literature.

References

[1] Jagger E. T., *Study of the Lubrication of Synthetic Rubber Rotary Shaft Seals*. Proceedings of the Conference on Lubrication and Wear, I.Mech.E., pp. 409-415, 1957.

[2] Müller, H.K., *Concepts of sealing Mechanism of Rubber Lip Type Rotary Shaft Seals*, Proceedings of the 11th International Conference on Fluid Sealing, B.H.R.A., Paper K1, pp. 698-709, 1987.

[3] Salant, R.F., *Numerical Analysis of the Flow Field Within Lip Seals Containing Microundulations*, ASME Journal of Tribology, Vol. 114, pp. 485-492, 1992.

[4] Stakenborg, M.J.L., *On the Sealing Mechanism of Radial Lip Seals*, Tribology International, Vol. 21, pp. 335-340, 1988.

[5] Stakenborg, M.J.L., van Leeuwen, H.J. and ten Hagen E.A.M., *Visco-Elastohydrodynamic(VEHD) Lubrication in Radial Lip Seals: Part I - Steady-State Dynamic Viscoelastic Seal Behavior*, ASME Journal of Tribology, Vol. 112, pp. 578-583, 1990.

[6] van Leeuwen, H.J., and Stakenborg M.J.L., *Visco-Elastohydrodynamic (VEHD) Lubrication in Radial Lip Seals: Part 2 - Fluid Film Formation*, ASME Journal of Tribology, Vol. 112, pp. 584-592, 1990.

[7] M. Amabili, G. Colombo and E. Prati, *Leakage of Radial Lip Seals at Large Dynamic Eccentricities*. Proceedings of the 16th International Conference on Fluid Sealing, September 18-20, Brugge, Belgium, pp. 321-333, 2000.

[8] M. Amabili, G. Colombo and E. Prati, *On the Leakage of Radial Lip Seals*. Proceedings of 2000 AIMETA International Tribology Conference, 20-22 September, LAquila, Italy, pp. 565- 572, 2000.

[9] M.Silvestri, E.Prati, A.Tasora, *Dynamic Seals Behaviour under Effect of Radial Vibration*, 14th International Colloquium Tribology, Esslingen (Stuttgart), Germany, January 13-15 2004, ISBN 3-924813-54-X, pp. 1247-1254

[10] M.Silvestri, E.Prati, A.Tasora, *Numerical Analysis of Sealing Conditions in Elastomeric Rings*, IV Aimeta International Tribology Conference Proceedings, Rome, Italy, September 14-17 2004, ISBN 88-7999-831-5, pp. 509-606.

[11] M.Silvestri, E.Prati, A.Tasora, *Numerical and experimental study of dynamic elastomeric seals behaviour under actively controlled temperature conditions*, Proceedings of 18th International Conference on Fluid Sealing, Antwerp, Belgium, October 12-14, 2005.

[12] F.Shi, R.F.Salant, *Numerical study of a rotary lip seal with a quasi-random sealing surface*, ASME Journal of Tribology, Vol. 123, pp. 517-524, 2001.

[13] A.A.Elsharkawy, *Visco-elastohydrodynamic lubrication of line contacts*, Wear, Vol. 199, pp. 45-53, 1996.
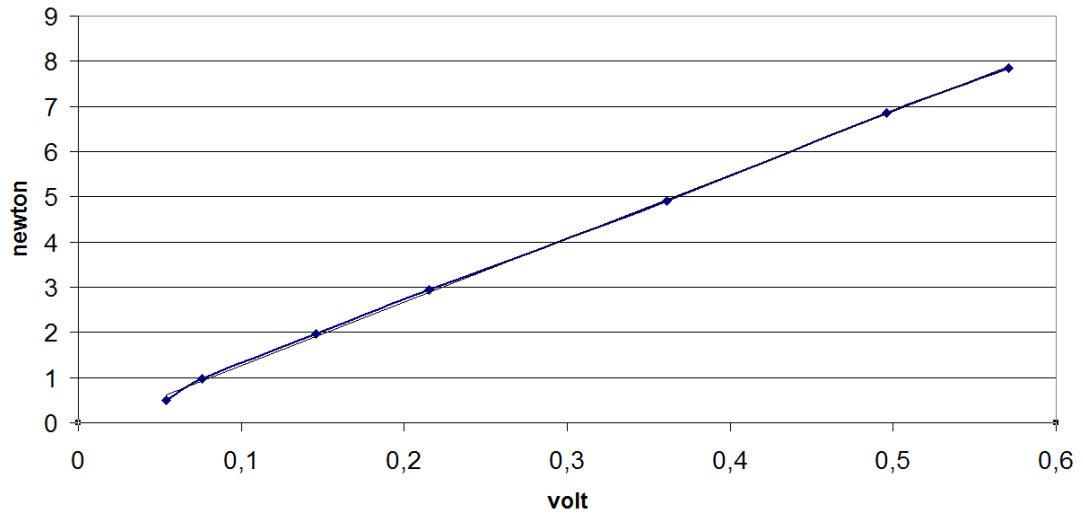
Figure 1: Transducer calibration curve.
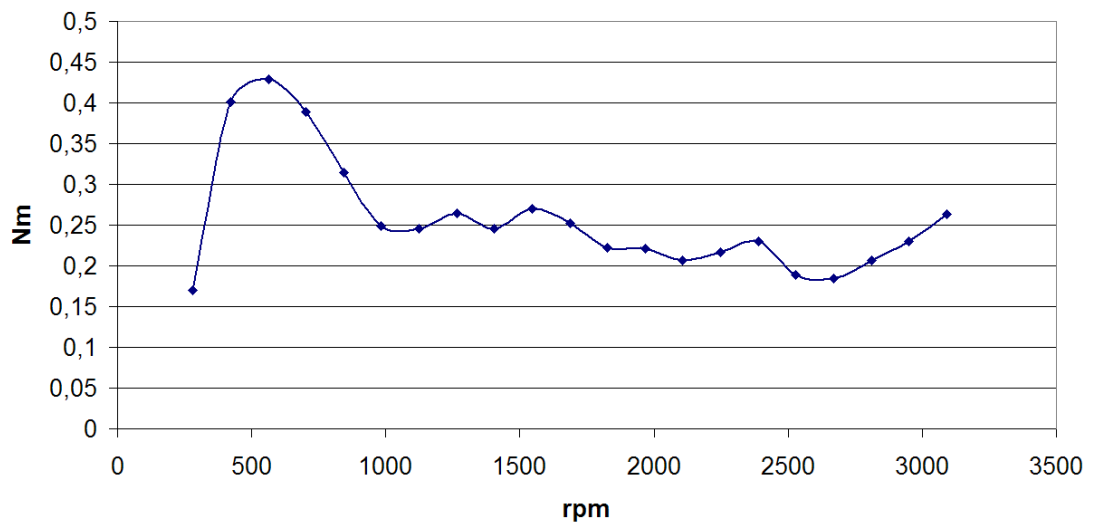
Figure 2: Friction torque at varying shaft speed.
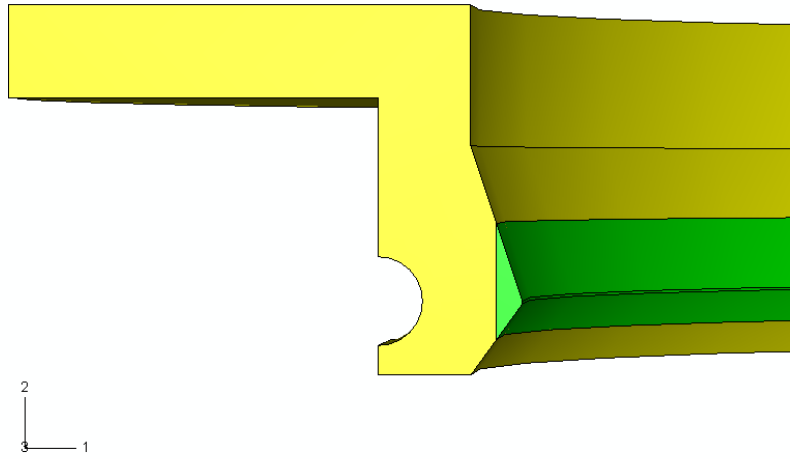
Figure 3: Seal model partition.
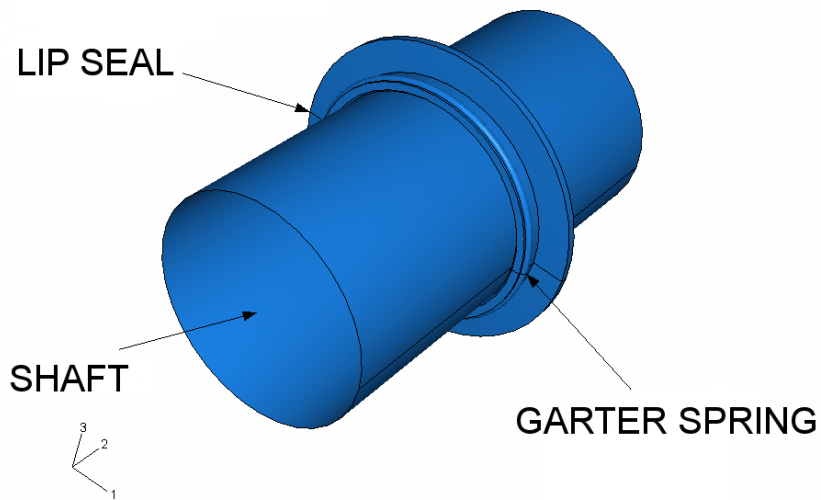
Figure 4: Shaft, seal and spring assembly.
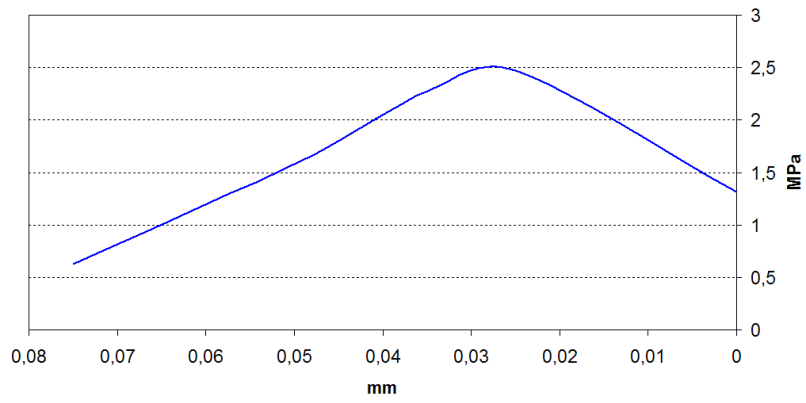
Figure 5: Normal stress on the lip surface.
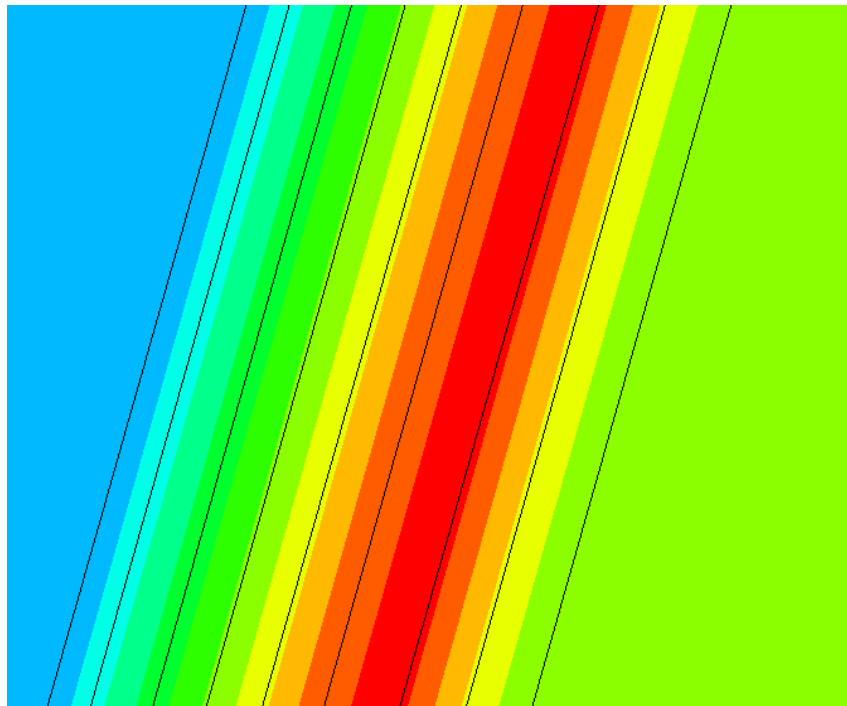
Figure 6: Normal stress on the lip surface.
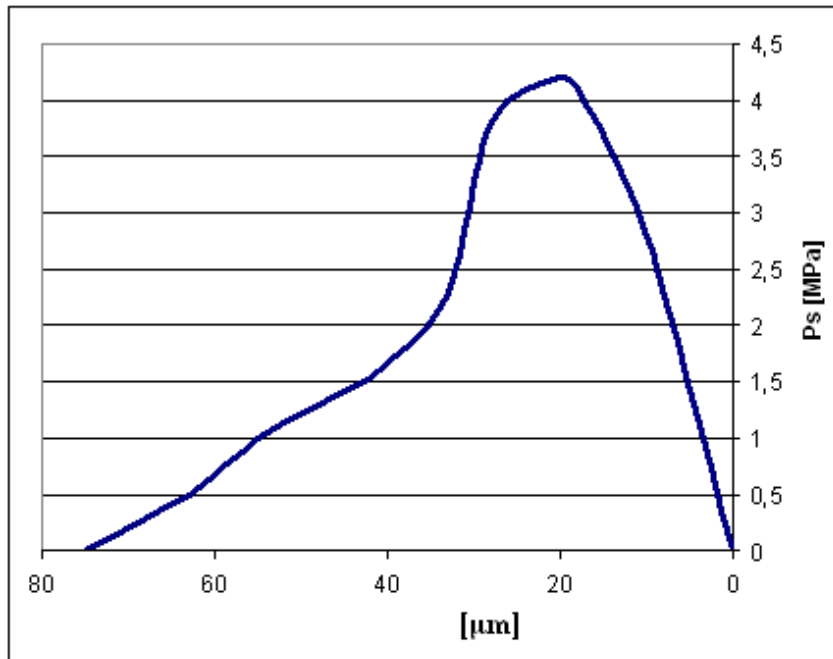
Figure 7: Normal stress calculated by [5].
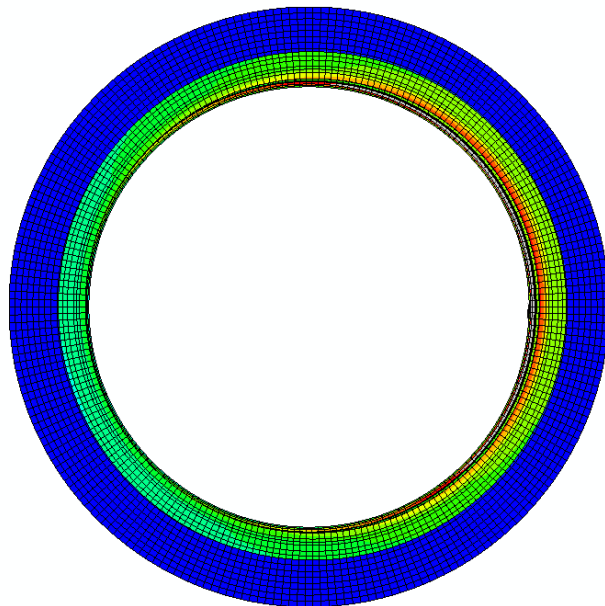
Figure 8: Lip strains in presence of eccentricity.
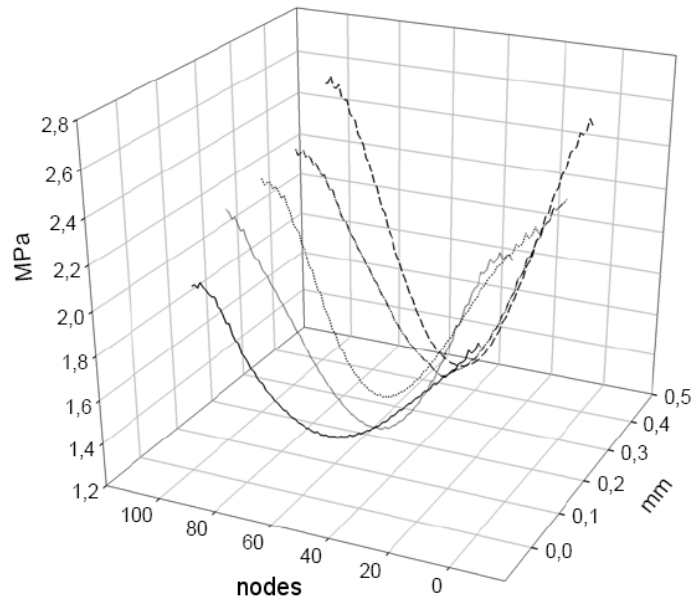
Figure 9: Normal stress around the shaft at varying ε_d.
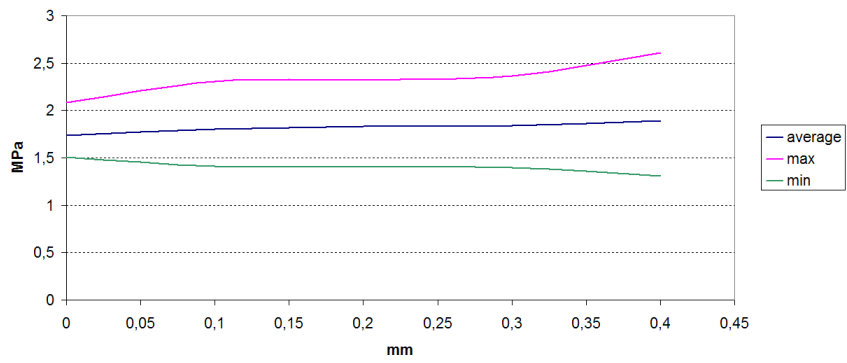
Figure 10: Max, average and min normal stress at varying ε_d.
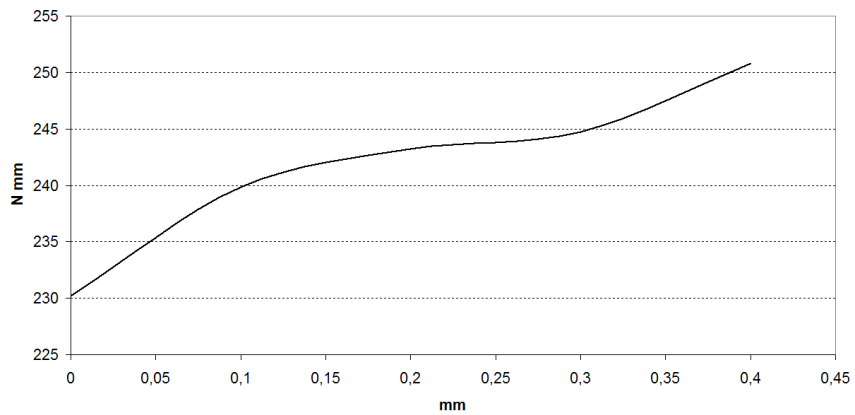
Figure 11: Friction torque at varying ε_d.
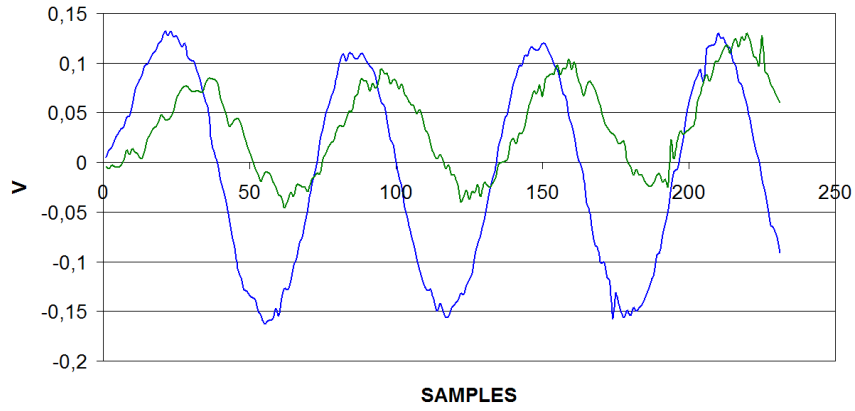
Figure 12: Tangential and radial lip strains at 350 rpm.
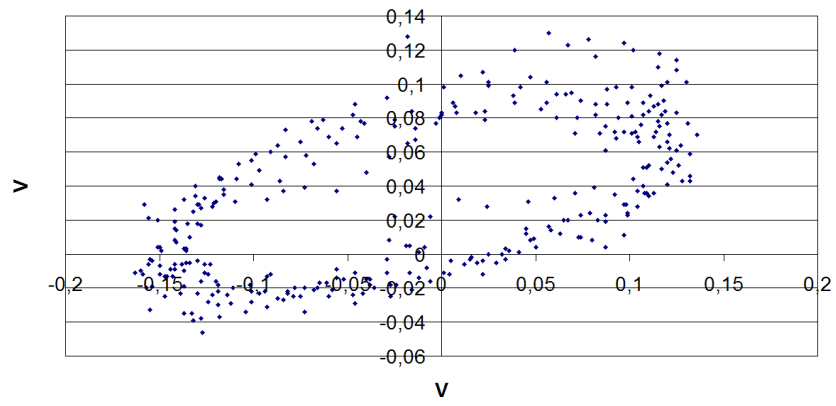
Figure 13: Tangential and radial lip strains at 350 rpm.
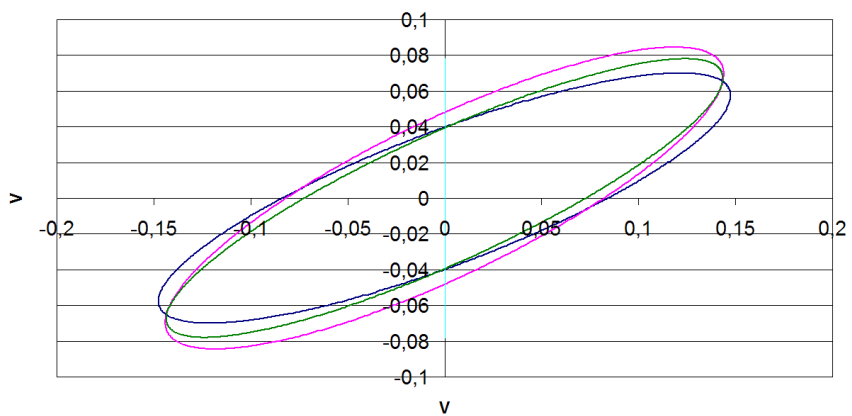
Figure 14: Interpolated ellipses. (Data at 350 rpm)
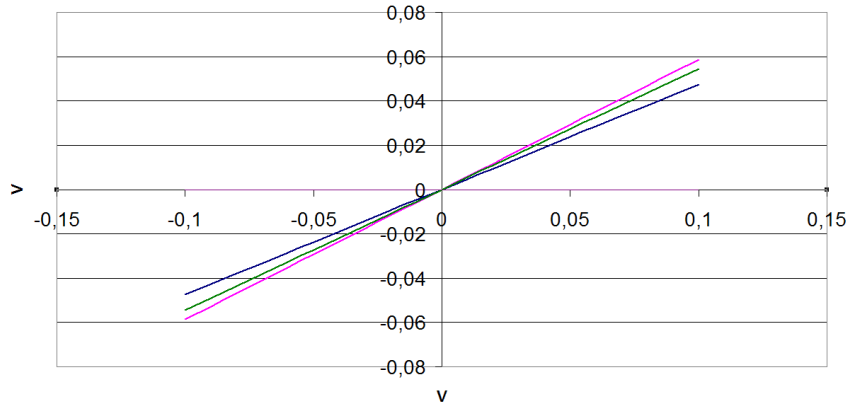
Figure 15: Ellipses major axis slope. (Data at 350 rpm)
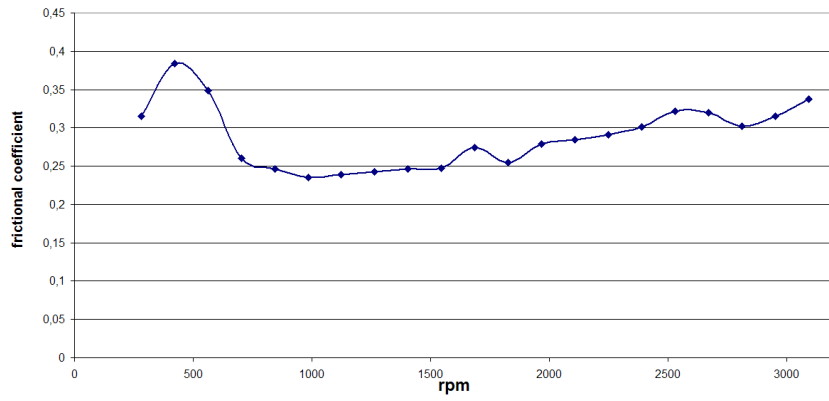
Figure 16: Friction coefficient indirect estimate.
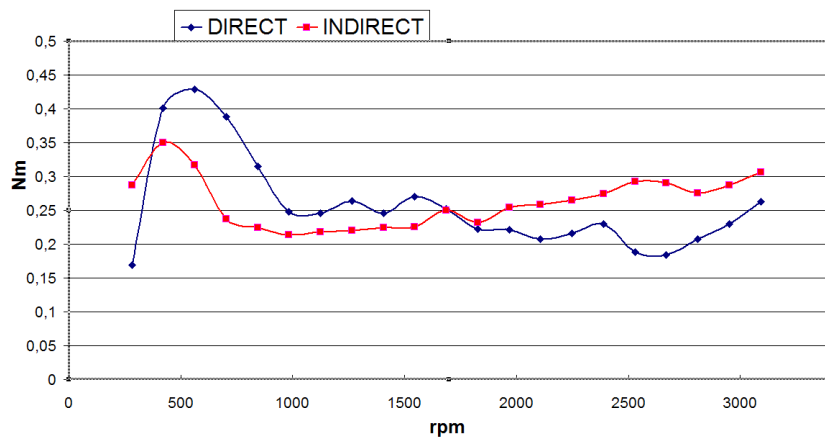
Figure 17: Direct and indirect friction torque measures.